

pubs.acs.org/joc Note

# Photoactivated Pyridine Directed Fluorination through Hydrogen Atom Transfer

Eric Holt, Jonah Ruskin, Nathaniel G. Garrison, Srini Vemulapalli, Winson Lam, Neil Kiame, Nicolas Henriquez, Fanny Borukhova, Jack Williams, Travis Dudding,\* and Thomas Lectka\*



Cite This: J. Org. Chem. 2023, 88, 17538–17543



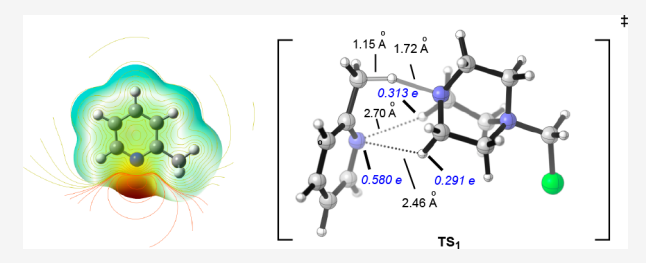
**ACCESS** I

Metrics & More

Article Recommendations

SI Supporting Information

ABSTRACT: We have established hydrogen atom transfer (HAT) as the key player in a directed, photopromoted fluorination of pyridylic groups. The Lewis basic pyridyl nitrogen directs amine radical dication propagated HAT and Selectfluor fluorination of various ortho substituents in a highly regioselective manner with little to no side product formation. A variety of pyridines and quinolines were employed to showcase the directing capability of the nitrogen atom. Additionally, both experimental and computational data are provided that illuminate how this mechanism differs from and complements prior work in the area.



The timely subject of selective benzylic fluorination both well-documented and well-understood mechanistically. Known art on analogous pyridylic fluorination is in contrast relatively sparse and much less understood. In this Note, we present a general fluorination protocol for pyridylic systems that proceeds through a defined hydrogen atom transfer (HAT) process to yield a variety of products in good to excellent yields and high regioselectivity. Most notably, the reaction possesses a directed component in which the pyridine nitrogen forms a putative nonclassical H-bonding interaction with the HAT reagent to direct the reaction predominately to the 2-position (Scheme 1).

Scheme 1. Basic Reaction Scheme

The literature on pyridine fluorination displays a wide variety of approaches over any systemic pattern. Several procedures involve the fluorination of the pyridine ring itself, whereas another approach employs a neat deprotonation protocol to access the fluorination of para-benzylic sites. However, there exist two papers of interest to our present study. Chausset-Boissarie et al. and van Humbeck et al. both report a variety of substituted pyridines that react directly with Selectfluor (and occasionally metal promoters) through a putative charge transfer complex. It should be noted, however, that our group has previously published experimental data demonstrating that the interaction between the lone pair of pyridine and Selectfluor is through the N···H—C bond rather

than the N···F–N halogen interaction, suggesting that a similar interaction may in some cases control pyridylic fluorination. Nonetheless, the precedented fluorinations occur at both ortho and para sites through either a postulated single-electron transfer (SET) or concerted proton-coupled electron transfer (PCET) pathway over the course of 16 and 20 h. It occurred to us that our recent work on site-selective, directed fluorination could as well be brought to bear on this problem through a clear-cut, documented mechanistic pathway that would as well provide predictive value for substrate elaboration. Previously, our group has reported on the ability of the carbonyl groups of enones, ketones, and the hydroxy groups of alcohols to direct the fluorination of aliphatic carbons through a HAT mechanism with benzil as photoactivator and Selectfluor as fluorinating agent (Scheme 2).

The initial discovery was made in a circuitous manner. One of the inherent features of our radical based reactions has been the production of HF as a byproduct in some cases. In the past we would typically employ 1 to 2 equiv of NaHCO<sub>3</sub> to basify the reaction; however, NaHCO<sub>3</sub> has poor solubility in organic solvents such as acetonitrile, and cloudy solutions can seriously hamper the effectiveness of a photoactivated reaction. To work around this, we investigated the use of organic bases in the fluorination of the test substrate, menthone (1). We employed 2,6-dimethylpyridine (2) in one run; to our surprise, when 1

Received: September 20, 2023 Revised: October 31, 2023 Accepted: November 13, 2023 Published: November 30, 2023





#### Scheme 2. Established Directed Fluorination

## previously published findings

$$\begin{array}{c} \begin{array}{c} \begin{array}{c} \\ \\ \\ \\ \end{array} \end{array} \begin{array}{c} \\ \\ \\ \end{array} \begin{array}{c} \\ \\ \end{array} \begin{array}{c} \\ \\ \\ \\ \end{array} \begin{array}{c} \\ \\ \\ \\ \end{array} \begin{array}{c} \\ \\ \\ \\ \end{array} \begin{array}{c} \\ \\ \\ \end{array} \begin{array}{c} \\ \\ \\ \end{array} \begin{array}{c} \\ \\ \\ \\ \end{array} \begin{array}{c} \\ \\ \\ \\ \end{array} \begin{array}{c} \\ \\ \\ \\ \end{array}$$

#### Z = directing group

(0.25 mmol) was subjected to benzil (0.2 equiv), Selectfluor (1.0 equiv), and **2** (1.0 equiv) we observed pyridyl fluorination exclusively (as a mixture of mono- and difluorinated products). Moreover, 2,4,6-trimethylpyridine (3) was subjected to our reaction and once again we found fluorination of specifically the ortho methyl groups (Scheme 3).

In light of our experience, we presumed that the reaction proceeded through a HAT pathway, although the (SET and/or PCET) results of Chausset-Boissarie and Humbeck et al. made

## Scheme 3. Initial Findings Leading to the Present Study

### initial observation

#### selective fluorination at ortho positions

#### SRD generation test

# H-bonding of pyridine and SRD

# Fluorination of pyridine

us pause. First, we considered the possibility that pyridine reacts with Selectfluor to form the Selectfluor derived radical dication (SRD),<sup>12</sup> so we replaced benzil with pyridine and tested several ketones, including 1, that we had previously shown to undergo directed fluorination<sup>13</sup> (Scheme 3). None of them were found to fluorinate to any extent, making it unlikely that pyridine promotes the formation of SRD under these conditions. In Scheme 4, we show a series of competition

# Scheme 4. Competition Experiments<sup>a</sup>

"Rate measurements were run to low conversion and extrapolation to zero conversion; standard procedure (SP) = 0.125 mmol substrate(s), 0.2 equiv of benzil, 0.2 equiv of NaHCO<sub>3</sub>, 0.7 equiv of Selectfluor in 1.0 mL of MeCN, 15 min of irradiation, stirring for 30 min total for all runs unless stated otherwise. Reactions were monitored by F-NMR. (a) SP. (b) SP. (c) SP. (d) SP. (e) 1.0 equiv of DABCO ammonium derivative added to SP. (f) 0.25 eq 4 used with SP. (g) SP with visible light (without light run overnight, as product formation is trace in 30 min).

reactions that shed light on a potential reaction pathway (Full experimental details given on S3). First, when comparing 2-methylpyridine (4) to its trideuterated counterpart (5) in (a), we measured a KIE value of 2.9, which is consistent with a typical primary KIE for related HAT processes (calcd. at IEFPCM (solvent = MeCN)  $\omega$ B97X-D/6-31+G(d,p), KIE = 2.3) although it does not differentiate between HAT and SET/PCET.

Next, we compared the rate of the fluorination of 4 to 4-methylpyridine (6) in (b) and found 9:1 selectivity in the formation of product 4F (we believe that the residual para fluorination is a result of the competing PCET/SET reaction). Then we compared the fluorination of toluene (7) to 4 and 6 (c, d). Both 4 and 6 fluorinate faster than 7, but in the case of

6 the difluorinated product was observed predominately. Additionally, we measured the rate of reaction in the presence of various excess equivalents of base, including a DABCO ammonium derivative and 1 equiv of 4. The thought was that in the advent of a PCET mechanism, the rate of reaction should increase exponentially. In all cases we found the effect of excess base to be negligible (with the DABCO derivative) (e) or else to provide a linear increase in the rate (with the pyridine substrate) (f). Finally, in an important and highly illuminating finding, we subjected 8 to standard conditions and found that without light (analogous to prior art) product 8F is favored (g), but to a much smaller degree, 2.1:1, compared to the photoactivated pathway (>99:1), demonstrating that the formation of SRD is key for a high degree of selectivity. The decoupled <sup>19</sup>F NMR demonstrating this regioselectivity can be found on S5.

Scheme 5 shows an optimization table for the fluorination of 9, wherein we discovered the practical benefit of short

Scheme 5. General Reaction Scheme for Fluorinations and Light Exposure Results<sup>a</sup>

general fluorination scheme

light exposure (min.)	yield
0	5
5	42
10	47
15	60
20	43
25	36
30	34
120	33

<sup>a</sup>Prolonged light exposure results in HF production, thus lowering yields.

irradiation times. Additional optimization data demonstrate the utility of adding additional portions of Selectfluor as the reaction progresses (S#). Scheme 6 shows a number of directed examples (generally, the reaction produces only trace amounts of other isomers that were not isolated). The scope of the reaction excludes alkoxy groups (ring fluorination) and halogens in the ortho positions (due to deactivation).

Quinoline derivatives performed best under the reaction conditions (Scheme 6); they appear in numerous different pharmaceutical compounds<sup>14</sup> and are therefore of interest to the medicinal chemistry community. This includes 23F, a deactivated quinoline that is incapable of being fluorinated using just Selectfluor,<sup>15</sup> likely because the quinoline is less likely to be activated through the PCET/SET mechanism. Finally, we tested our fluorination on a pharmaceutical compound, etoricoxib<sup>16</sup> (Scheme 7), which forms product in 67% yield.

In order to provide additional support for HAT reactivity, we performed density functional theory (DFT) calculations using 2-methyl pyridine (4), toluene (7), and open-shell dicationic radical SRD as model substrates. <sup>17</sup> Initial transition state (TS) searches located the lowest energy HAT transition

Scheme 6. General Table<sup>a</sup>

"Yields determined by <sup>19</sup>F-NMR relative to internal standard. Yields based on recovered starting material given in parentheses.

Scheme 7. Fluorinated Etoricoxib

state structures  $TS_1$  and  $TS_2$  with Gibbs free activation energies (DG<sup>‡</sup>) of 4.1 and 7.5 kcal/mol relative to SRD and the individual substrates to generate intermediates INT-1 and INT-2. In terms of TS<sub>1</sub>, attack of radical dication SRD at the methyl group C-H bond located proximal to the pyridine nitrogen occurs with bond breaking and bond making distances of 1.15 and 1.72 Å (Figure 1a). In this case, the transferring hydrogen carries a calculated partial positive charge of 0.376 e, which is not unusual for HAT.<sup>18</sup> As for potential inner-sphere PCET involving the nearby pyridine group, the theoretical criteria of Mayer and co-workers disfavor this possibility. 19 Stepwise electron transfer/proton transfer (ET/PT) processes involving SRD are also disfavored based on our KIE study.<sup>20</sup> As a point of comparison, the transition state for HAT from 4-methyl pyridine is 7.2 kcal, slightly less than that for toluene (see Supporting Information for details).

The SOMO and computed open-shell spin density of transition state **TS**<sub>1</sub> is consistent with HAT-type C-H bond cleavage (Figure 1b, *left-hand side*). The directing effect of the pyridine nitrogen lone pair in guiding HAT is also notable, as

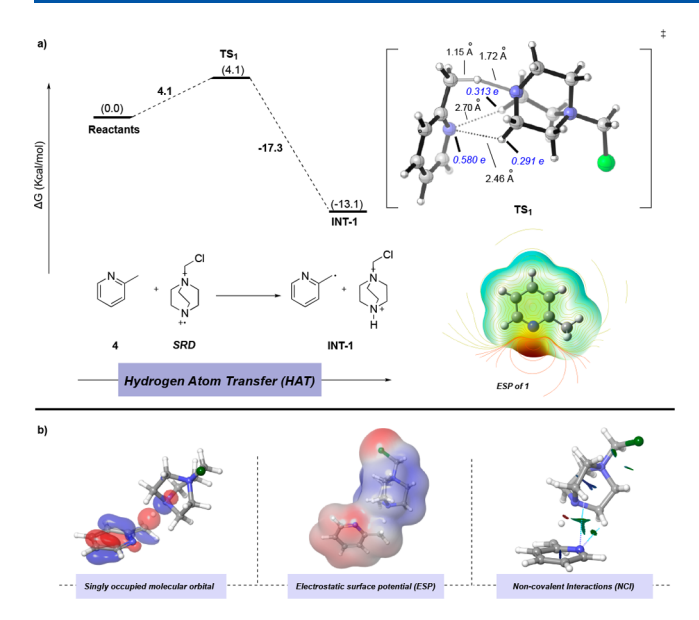


**Figure 1.** (a) Hydrogen atom transfer (HAT) pathway of 4 computed at the (IEFPCM = MeCN) wB97XD/6-31+G(d,p) level of theory with NBO charges of H7, H12, and N38 highlighted. (b) Singly occupied molecular orbital (SOMO) (left-hand side), electrostatic surface potential (ESP) (middle), and noncovalent interaction (NCI) plot of  $TS_1$  (right-hand side).

seen from the electrostatic surface potential (ESP) map (Figure 1b, middle). An NCI plot of TS<sub>1</sub> reveals stabilizing noncovalent interactions (Figure 1b, right-hand side, green shaded area) linked to nitrogen lone pair steering. This effect is supported by hydrogen bond C-H···N contacts measuring 2.46 and 2.70 Å, with columbic character as gauged by natural bond order (NBO) charges (N = -0.580 e, H = +0.291 e, H = +0.313 e). Furthermore, Quantum Theory of Atoms in Molecules (QTAIM) computations unveiled (+3, -1) bond critical points (bcp) with positive rho (r) and Laplacian  $(\nabla 2\rho)$ values ( $\rho$ bcp = 0.0047 au, 0.0072 au and  $\nabla 2\rho$ bcp = 0.0155 au, 0.0221 au) associated with these C-H···N interactions (Figure 2 or see Supporting Information for details). These interactions and ascribed values are indicative of moderate hydrogen bonding between SRD and the nitrogen lone-pair of pyridine with electrostatic or polarization contributions. Likewise, the relief map of  $\nabla 2\rho$  supports these ionic characteristics of these hydrogen bonds as seen from regions of charge depletion on the contour map.

In contrast, C–H abstraction of toluene occurs with bond-breaking and bond-making distances of 1.11 and 2.19 Å through TS<sub>2</sub> (Figure 3a). The SOMO (Figure 3b, left-hand side) and open-shell spin of this transition state were indicative of C–H bond cleavage by HAT with a small degree of positive charge buildup of +0.240 e on the transferring hydrogen (Figure 3b, middle). Furthermore, steric interactions were no factor. The basis for HAT being higher energy in this instance is ascribed to a lack of nitrogen lone pair directing group participation, thus yielding a higher TS energy value.

In conclusion, we have successfully employed a photoactivated HAT reaction for the pyridine nitrogen directed fluorination of aliphatic carbons. The mechanism was postulated through a variety of different competition experiments and backed by computational data. Additionally, the reaction was demonstrated to work well on a variety of different pyridine and quinoline derivatives as well as a



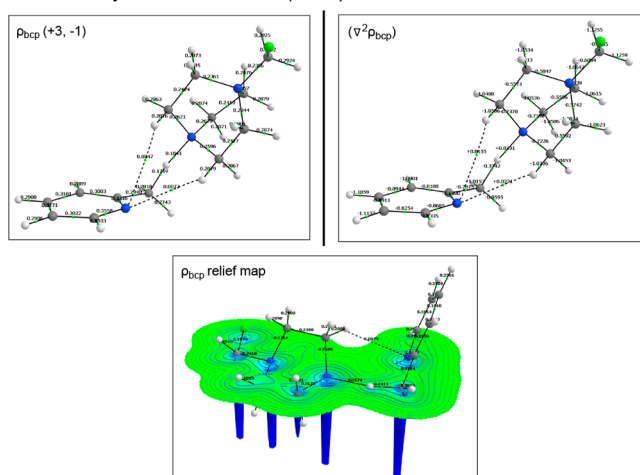
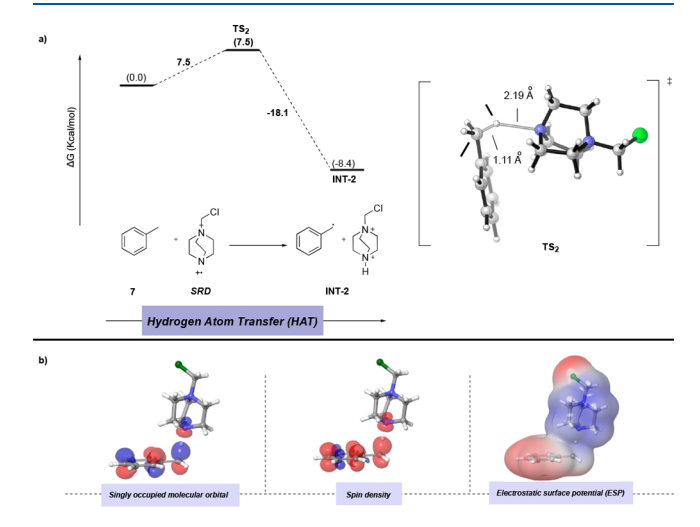


Figure 2. Quantum theory of atoms in molecules (QTAIM) analysis of TS<sub>1</sub> computed at the wB97X-D/6-31+G(d,p) displaying the (+3, -1) bond critical point  $\rho_{\rm bcp}$  (left), the Laplacian  $\nabla^2\rho_{\rm bcp}$  of the bcp (middle) and a relief map of the  $\rho_{\rm bcp}$  depicting the electron density of TS<sub>1</sub> (right).



**Figure 3.** (a) Hydrogen atom transfer (HAT) pathway of toluene 4 computed at the (IEFPCM = MeCN) wB97XD/6-31+G(d,p) level of theory. (b) Singly occupied molecular orbital (SOMO (left), spin density plot (middle), and electrostatic surface potential (ESP) of  $TS_2$  (right).

pharmaceutical compound currently in use. Future studies will aim at expanding the capability and applicability of this reaction.

## ASSOCIATED CONTENT

# **Data Availability Statement**

The data underlying this study are available in the published article and its Supporting Information.

## **Supporting Information**

The Supporting Information is available free of charge at https://pubs.acs.org/doi/10.1021/acs.joc.3c02146.

Experimental procedures, spectra, and computational data (PDF)

#### AUTHOR INFORMATION

## **Corresponding Authors**

Thomas Lectka — Department of Chemistry, Johns Hopkins University, Baltimore, Maryland 21218, United States; orcid.org/0000-0003-3088-6714; Email: lectka@jhu.edu

Travis Dudding — Department of Chemistry, Brock University, St. Catharines, Ontario L2S3A1, Canada; ⊕ orcid.org/0000-0002-2239-0818; Email: tdudding@brocku.ca

#### **Authors**

Eric Holt — Department of Chemistry, Johns Hopkins University, Baltimore, Maryland 21218, United States; orcid.org/0000-0003-2068-6962

Jonah Ruskin – Department of Chemistry, Johns Hopkins University, Baltimore, Maryland 21218, United States; orcid.org/0009-0006-4422-8535

Nathaniel G. Garrison – Department of Chemistry, Johns Hopkins University, Baltimore, Maryland 21218, United States

Srini Vemulapalli — Department of Chemistry, Brock University, St. Catharines, Ontario L2S3A1, Canada Winson Lam — Department of Chemistry, Johns Hopkins University, Baltimore, Maryland 21218, United States

Neil Kiame – Department of Chemistry, Johns Hopkins University, Baltimore, Maryland 21218, United States

Nicolas Henriquez – Department of Chemistry, Johns Hopkins University, Baltimore, Maryland 21218, United States

Fanny Borukhova — Department of Chemistry, Johns Hopkins University, Baltimore, Maryland 21218, United States Jack Williams — Department of Chemistry, Johns Hopkins

University, Baltimore, Maryland 21218, United States

Complete contact information is available at: https://pubs.acs.org/10.1021/acs.joc.3c02146

## Notes

The authors declare no competing financial interest.

# ACKNOWLEDGMENTS

T.L. thanks the National Science Foundation (NSF) (Grant No. CHE 2102116) for financial support. Mass spectral data were obtained at University of Delaware's mass spectrometry centers. T.D. thanks the Natural Sciences and Engineering Research Council of Canada for Discovery Grants (RGPIN-2019-04205). This research was enabled in part by the support provided by SHARCNET (Shared Hierarchical Academic Research Computing Network) and Compute/Calcul Canada and the Digital Research Alliance of Canada.

# REFERENCES

(1) (a) Groendyke, B. J.; AbuSalim, D. I.; Cook, S. P. Iron-Catalyzed, Fluoroamide-Directed C-H Fluorination. *J. Am. Chem. Soc.* **2016**, *138*, 12771–12774. (b) Nodwell, M. B.; Bagai, A.; Halperin, S. D.; Martin, R. E.; Knust, H.; Britton, R. Direct photocatalytic fluorination of benzylic C-H bonds with N-fluorobenzenesulfonimide. *Chem. Commun.* **2015**, *51*, 11783–11786. (c) Zhang, Q.; Mixdorf, J. C.; Reynders, G. J.; Nguyen, H. M. Rhodium-catalyzed benzylic fluorination of trichloroacetimidates. *Tetrahedron.* **2015**, *71*, 5932–5938. (d) Xia, J.; Zhu, C.; Chen, C. Visible Light-Promoted Metal-Free C-H Activation: Diarylketone-Catalyzed Selective Benzylic Mono- and Difluorination. *J. Am. Chem. Soc.* **2013**, *135*, 17494–17500. (e) Vasilopoulos, A.; Golden, D. L.; Buss, J. A.; Stahl, S. S.

- Copper-Catalyzed C-H Fluorination/Functionalization Sequence Enabling Benzylic Cross Coupling with Diverse Nucleophiles. *Org. Lett.* **2020**, *22*, 5753–5757. (f) Bloom, S.; McCann, M.; Lectka, T. Photocatalyzed Benzylic Fluorination: Shedding "Light" on the Involvement of Electron Transfer. *Org. Lett.* **2014**, *16*, 6338–6341.
- (2) Hua, A. M.; Bidwell, S. L.; Baker, S. I.; Hratchian, H. P.; Baxter, R. D. Experimental and Theoretical Evidence for Nitrogen-Fluorine Halogen Bonding in Silver-Initiated Radical Fluorinations. *ACS Catal.* **2019**, *9*, 3322–3326.
- (3) Pikun, N. V.; Sobolev, A.; Plotniece, A.; Rucins, M.; Vigante, B.; Petrova, M.; Muhamadejev, R.; Pajuste, K.; Shermolovich, Y. G. Synthesis of Fluorinated 3,6-Dihydropyridines and 2-(Fluoromethyl)-pyridines by Electrophilic Fluorination of 1,2-Dihydropyridines with Selectfluor. *Molecules.* **2020**, *25*, 3143.
- (4) Meanwell, M.; Nodwell, M. B.; Martin, R. E.; Britton, R. A Convenient Late-Stage Fluorination of Pyridylic C-H Bonds with N-Fluorobenzenesulfonimide. *Angew. Chem.* **2016**, *55*, 13244–13248.
- (5) Le Guen, C.; Mazzah, A.; Penhoat, M.; Melnyk, P.; Rolando, C.; Chausset-Boissarie, L. Direct and Regioselective C(sp³)-H Bond Fluorination of 2-Alkylazaarenes with Selectfluor. *Synthesis* **2021**, *53*, 1157–1162.
- (6) Danahy, K. E.; Cooper, J. C.; Van Humbeck, J. F. Benzylic Fluorination of Aza-Heterocycles Induced by Single-Electron Transfer to Selectfluor. *Angew. Chem.* **2018**, *57*, 5134–5138.
- (7) Mulliken, R. S. Charge-transfer band of the pyridine-iodine complex. J. Am. Chem. Soc. 1969, 91, 1237.
- (8) Capilato, J.; Harry, S. A.; Siegler, M.; Lectka, T. Spectroscopic and Crystallographic Characterization of the R3N+-C-H—X Interaction. *Chem.—Eur. J.* **2022**, No. e2021039.
- (9) Ghorbani, F.; Harry, S. A.; Capilato, J. N.; Pitts, C. R.; Joram, J.; Peters, G. N.; Tovar, J. D.; Smajlagic, I.; Siegler, M. A.; Dudding, T.; Lectka, T. Carbonyl-Directed Aliphatic Fluorination: A Special Type of Hydrogen Atom Transfer Beats Out Norrish II. *J. Am. Chem. Soc.* **2020**, *142*, 14710–14724.
- (10) Bume, D. D.; Pitts, C. R.; Ghorbani, F.; Harry, S. A.; Capilato, J. N.; Siegler, M. A.; Lectka, T. Ketones as directing groups in photocatalytic sp<sup>3</sup> C-H fluorination. *Chem. Sci.* **2017**, *8*, 6918–6923.
- (11) Harry, S. A.; Xiang, M. R.; Holt, E.; Zhu, A.; Ghorbani, F.; Patel, D.; Lectka, T. Hydroxy-directed fluorination of remote unactivated C(sp<sup>3</sup>)-H bonds: a new age of diastereoselective radical fluorination. *Chem. Sci.* **2022**, *13*, 7007–7013.
- (12) Madani, A.; Anghileri, L.; Heydenreich, M.; Moller, H. M.; Pieber, B. Benzylic Fluorination Induced by a Charge-Transfer Complex with a Solvent-Dependent Selectivity Switch. *Org. Lett.* **2022**, 24, 5376–5380.
- (13) Bume, D. D.; Pitts, C. R.; Ghorbani, F.; Harry, S. A.; Capilato, J. N.; Siegler, M. A.; Lectka, T. Ketones as directing groups in photocatalytic sp<sup>3</sup> C-H fluorination. *Chem. Sci.* **2017**, *8*, 6918–6923.
- (14) Yadav, P.; Shah, K. Quinolines, a perpetual, multipurpose scaffold in medicinal chemistry. *Bioorg. Chem.* **2021**, *109*, No. 104639.
- (15) Le Guen, C.; Mazzah, A.; Penhoat, M.; Melnyk, P.; Rolando, C.; Chausset-Boissarie, L. Direct and Regioselective C(sp³)-H Bond Fluorination of 2-Alkylazaarenes with Selectfluor. *Synthesis* **2021**, *53* (6), 1157–1162.
- (16) Salama, A. H.; Abdelkhalek, A. A.; Elkasabgy, N. A. Etoricoxibloaded bio-adhesive hybridized polylactic acid-based nanoparticles as an intra-articular injection for the treatment of osteoarthritis. *Int. J. Pharm.* **2020**, *578*, No. 119081.
- (17) Geometry optimization, vibration, and solvation energy calculations were performed at the (IEFPCM = MeCN) wB97XD/6-31+G(d,p) level of theory using the Gaussian 16 software package: Frisch, M. J.; Trucks, G. W.; Schlegel, H. B.; Scuseria, G. E.; Robb, M. A.; Cheeseman, J. R.; Scalmani, G.; Barone, V.; Mennucci, B.; Petersson, G. A.; Nakatsuji, H.; Caricato, M.; Li, X.; Hratchian, H. P.; Izmaylov, A. F.; Bloino, J.; Zheng, G.; Sonnenberg, J. L.; Hada, M.; Ehara, M.; Toyota, K.; Fukuda, R.; Hasegawa, J.; Ishida, M.; Nakajima, T.; Honda, Y.; Kitao, O.; Nakai, H.; Vreven, T.; Montgomery, J. A., Jr.; Peralta, J. E.; Ogliaro, F.; Bearpark, M.; Heyd, J. J.; Brothers, E.; Kudin, K. N.; Staroverov, V. N.; Kobayashi,

- R.; Normand, J.; Raghavachari, K.; Rendell, A.; Burant, J. C.; Iyengar, S. S.; Tomasi, J.; Cossi, M.; Rega, N.; Millam, J. M.; Klene, M.; Knox, J. E.; Cross, J. B.; Bakken, V.; Adamo, C.; Jaramillo, J.; Gomperts, R.; Stratmann, R. E.; Yazyev, O.; Austin, A. J.; Cammi, R.; Pomelli, C.; Ochterski, J. W.; Martin, R. L.; Morokuma, K.; Zakrzewski, V. G.; Voth, G. A.; Salvador, P.; Dannenberg, J. J.; Dapprich, S.; Daniels, A. D.; Farkas, Ö.; Foresman, J. B.; Ortiz, J. V.; Cioslowski, J.; Fox, D. J. Gaussian 16, Revision C.01; Gaussian, Inc.: Wallingford, CT, 2009.
- (18) Dilabio, G. A.; Franchi, P.; Lanzalunga, O.; Lapi, A.; Lucarini, F.; Lucarini, M.; Mazzonna, M.; Prasad, V. K.; Ticconi, B. Hydrogen Atom Transfer (HAT) Processes Promoted by the Quinolinimide-*N*-oxyl Radical. A Kinetic and Theoretical Study. *J. Org. Chem.* **2017**, 82, 6133–6141.
- (19) Weinberg, D. R.; Gagliardi, C. J.; Hull, J. F.; Murphy, C. F.; Kent, C. A.; Westlake, B. C.; Paul, A.; Ess, D. H.; McCafferty, D. G.; Meyer, T. J. Proton-Coupled Electron Transfer. *Chem. Rev.* **2012**, *112*, 4016–4093.
- (20) Darcy, J. W.; Koronkiewicz, B.; Parada, G. A.; Mayer, J. M. A Continuum of Proton-Coupled Electron Transfer Reactivity. *Acc. Chem. Res.* **2018**, *51*, 2391–2399.